HIGH ENERGY ELECTRON DETECTION WITH ATIC

J. Chang[1,2] **and W.K.H. Schmidt**[2]

For the ATIC collaboration

[1]Purple Mountain Observatory, Nanjing, China

[2]MPI f. Aeronomie, Lindau, Germany

Abstract.

The ATIC ballon borne ionization calorimeter is well suited to record and identify high energy cosmic ray electrons. The instrument was exposed to high-energy beams at CERN H2 beamline in September of 1999. We have simulated the performance of the instrument, and compare the simulations with actual high energy electron exposures at the CERN accelerator. Simulations and measurements do not compare exactly in detail, but overall the simulations have predicted actual measured behavior quite well.

1 Introduction

ATIC is an ionization calorimeter for the measurement of the composition and energy spectra of cosmic rays including heavy primaries up to very high energy (100TeV). A full description of the instrument can be found in these papers: Guzik, et al., 1999; Ganel, et al., 1999, Wefel, et al., 2001. It consists of a target of 3/4 proton interaction lengths (30 cm) of graphite followed by about 22 radiation lengths (25 cm, equivalent to about 1.1 proton interaction lengths) of Bismuth Germanate (BGO) scintillator. The graphite target (comprising only 1.6 radiation lengths) is there to force as many protons and heavier nuclei as possible to interact early in the instrument, so that the conditions for the ensuing shower development are similar for all events.

We have investigated the possibility to identify high energy primary cosmic ray electrons in the presence of the 'background' of cosmic ray protons by simulating nuclear electromagnetic cascade showers in the dense material of the calorimeter using the GEANT computer code (Brun et al., 1984). We find that the design consisting of a graphite target followed by an energy detection device, consisting of a totally active calorimeter built up of 2.5 cm x 2.5 cm x 25.0 cm BGO scintillator bars, gives us sufficient information to distinguish electrons from protons reasonably well. While identifying about 70% of electrons as such, only about one in 10,000 protons will mimic an electron (Schmidt et al., 1999).

In September 1999, ATIC was exposed to high-energy beams of protons and electrons of several energies from 100 GeV to 375 GeV at CERN (H2 beamline). Results have been reported by Ganel et al., 2000. We have analyzed these data and found that although measurements and simulations do not compare exactly in detail, overall the simulations have predicted actual measured behavior quite well. One has to keep in mind that simulation calculations are always exactly calibrated, while no instrument is perfect. The simulation and calibtration measurement results are reported in this paper.
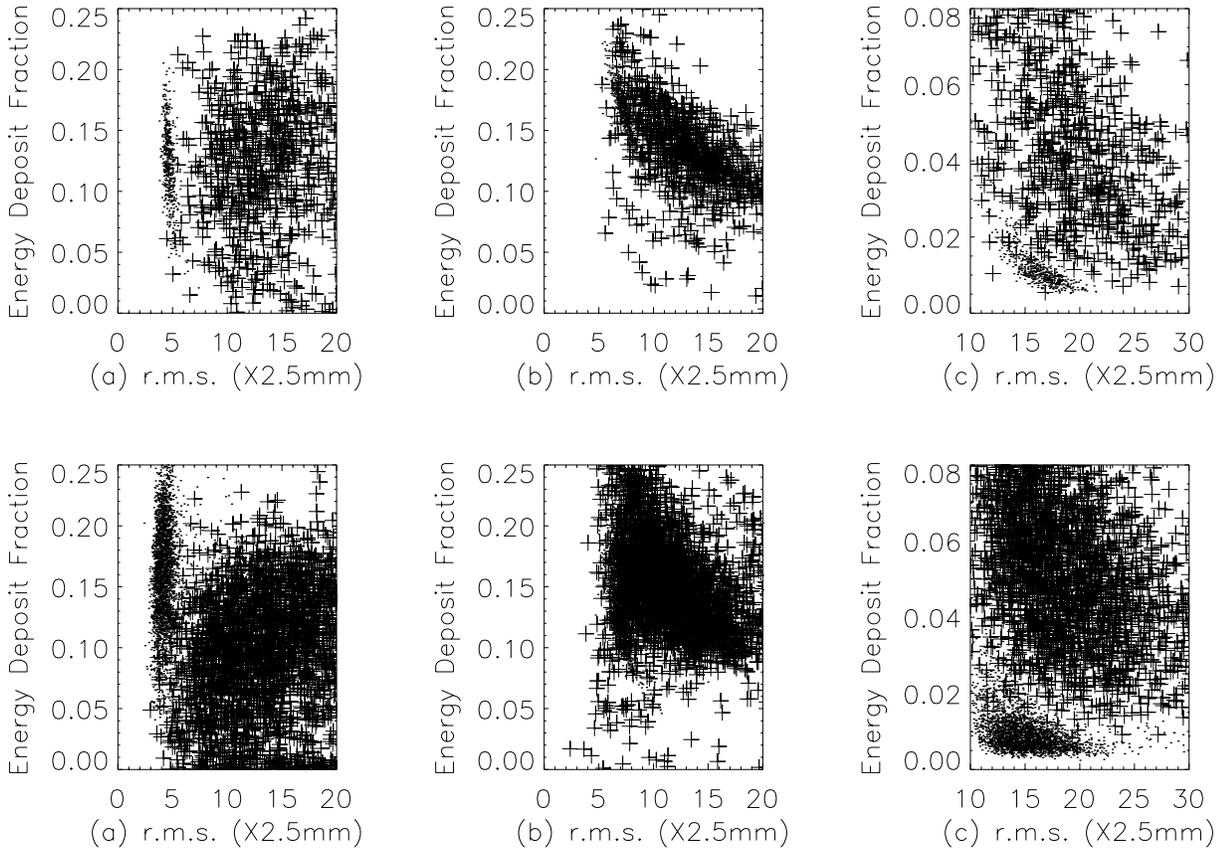
Fig. 1. Scatter plots for incident electrons and protons (+ proton events, . electron events). The top plots are from simulations, the bottom plots are from the experiment. For explanation see text.

2 The Shower Development in the ATIC

By simulation we find that primary electrons deposit about 95% of their energy in the BGO calorimeter while protons on average deposit about 40%. In this paper we always compare proton and electron events with the same total energy deposit in the calorimeter.

Figure 1 shows the difference of the shower development between electrons and protons. These are scatter plots of shower energy deposits of individual events vs widths of showers at three different depths in the BGO calorimeter (BGO2, BGO5 and BGO10, counting from just beneath the target).

On the ordinate the energy deposit in a particular BGO layer is expressed as a fraction of the total energy of that event assuming that it was an electron with average behavior, and the shower width is expressed as the r.m.s. value on the abscissa. The r.m.s. value is calculated in each individual layer around the scintillator bar with the highest energy deposit. The top row of plots are simulation results of 150 GeV electrons and 150 GeV-5 TeV protons where only events with energy deposit close to that of 150 GeV electrons were selected: 150 GeV electrons of the CERN beam

deposit on average about 139 GeV in the BGO calorimeter (this is less than in the simulations because of the finite width of the real beam and some positional dependence of the energy deposit); therefore, only proton events which deposited between 119 and 159 GeV in the calorimeter were used for comparison. The bottom row of plots are CERN exposure results of 150 GeV electrons and 375 GeV protons (again selected for energy deposit similar to the electrons).

It can be seen in Figure 1 that although the results of simulation and observation do not agree exactly, some major features of the simulations are reproduced in the data, markedly the separation and/or overlap of the scatterplot populations of electrons and protons. The differences are presumably due to slight differences in the average shower curves between simulation and observation, and some additional scatter is possibly due to calibration uncertainties. While near the top of the calorimeter (layer BGO2, Fig. 1a) the electron events and proton events form separate groups, these groups overlap more and more as the showers develop with increasing depth in the calorimeter. At the very bottom of the calorimeter the groups separate again. We use the method described by Schmidt et al. (1999) to distinguish events from incident electrons and protons.
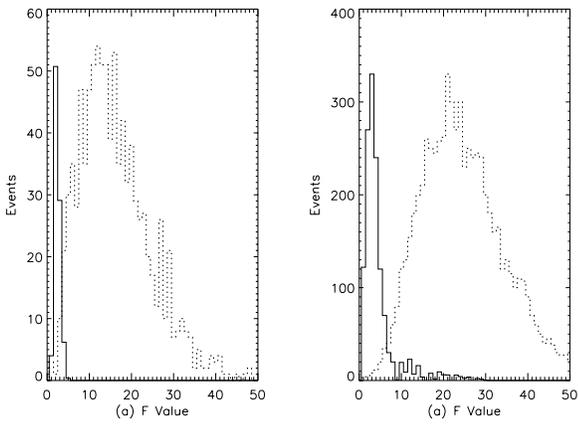
Fig. 3. F-Value distributions (see text) for incident electrons (solid line) and incident protons of comparable total energy deposit in the calorimeter (dashed line) for the signals in the last calorimeter layer BGO10. The left plot is from simulation, and the right plot is from the CERN exposure
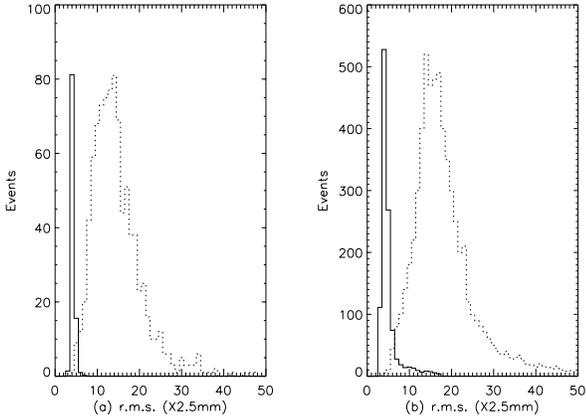

Fig. 2. Comparison of the widths of showers initiated by electrons (solid line) and protons (dashed line) as determined by the r.m.s.-value of signals about the shower axis in the BGO scintillator bars in the second BGO layer, BGO2. The left plot is from simulation calculations, and the right plot is from the CERN calibration experiment

3 Electron-Proton Distinction

First we make use of the lateral distribution of the energy deposit, i.e. the distribution of the widths of the showers in a particular layer of the calorimeter. Particularly the top calorimeter layer BGO2 shows good discrimination between electrons and protons as shown in Figure 2. Here the projected width of the shower around its axis is expressed by its r.m.s. value. The r.m.s.-value distributions of electron and proton events of the same total energy deposit (in the whole calorimeter) are well separated. Deeper in the calorimeter this separation is lost. From the CERN exposure results we find that 90% protons will be rejected by this step.

In a next step we look at the last layer BGO10. In Fig.1 we recognize that electron initiated events and proton initiated events again form separate groups, but it is not a simple r.m.s. value that distinguishes them. Therefore we define a function $F = (En/Sum) * r.m.s.^2$. If we plot the F-value distributions for BGO10 we obtain Figure 3. The separation of the distributions of proton and electron initiated events is about as good as in Figure 2. This again helps to suppress the proton 'background' from the point of view of electron observations. Incidentally, if the scatter plot of Figure 1c were taken by itself, about 99% of the proton events would be rejected in that step alone.

Further we compute the trajectory of the incoming particle from the three dimensional shower information inside the calorimeter. Then we try to fit the longitudinal shower curve of an event with a particular energy deposit to the average shower curve corresponding to an electron event of the same total energy deposit. By requiring a goodness of fit as expressed by $\chi^2 = 0.6$ per degree of freedom we lose several percent of the electrons but reject about 60% of the protons.

4 Results

From CERN experimental data, we have analyzed 8741 proton events and 3924 electron events. After the first step 42 protons and 3348 electron are kept, after the second step 6 protons and 3090 electrons are kept, after the last step only 3 protons remain looking like electrons, but 3034 electrons are kept. So the detection efficiency is about 77% and the rejection efficiency is about 0.9997.

Figure 4 shows the expected electron observation results and proton backgrounds. The proton spectrum is from Webber (1997), $J_p = 1.94 * 10^4 * E^{-2.75}/(m2*s*sr*GeV)$, and the electron spectrum is from Nishimura et al. (1980), $J_e = 5.72 * 10^2 * E^{-3.26}/(m2*s*sr*GeV)$. It can be seen that at 150 GeV only about 4% of the observed electrons are really incident proton background events. This agrees with the the simulation results very well; in the simulations this value is about 5%. In Fig. 4 it can also be seen that the proton background will increase slightly with increasing energy because of different spectral indices of the proton and electron spectra. Therefore at 1000 GeV about 10% of the events are from the proton background. However, according to the simulation result, the proton rejection power also increases with increasing energy; therefore we expect that between 500 GeV - 1000 GeV only 5% events are protons mimicking electrons.

5 Summary and Conclusions

We have described the results of simulation calculations and have compared them with actual exposures to high energy electrons and protons at CERN. We find that we can use ATIC to observe electrons among the abundant cosmic ray protons. Our approach is to take the calorimeter as it is, optimized for the detection of cosmic ray protons and heavier nuclei, so that the primary purpose of this experiment will
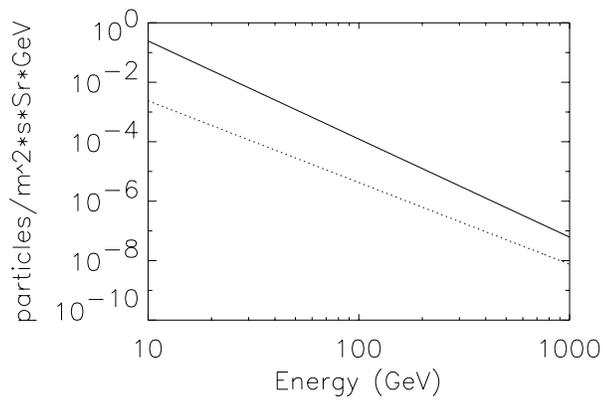
Fig. 4. The expected observational results for the cosmic ray electron spectrum (solid line) and proton background contained therein (dashed line)

not be compromised. ATIC was launched as a long duration ballon test flight on 2000/12/28 for a 16 day flight (384 hours of data taking) from McMurdo, Antarctica. The data analysis is in progress, and the preliminary results on the electron spectrum will be reported later.

References

Brun,R., et al., GEANT Handbook, CERN DD/EE/84-1 (Geneva) 1984

Ganel, O., et al., Proc. 26th ICRC(Salt Lake City 1999), paper code OG 4.6.01

Ganel, O., et al., First Results from ATIC Beam-test at CERN, advances in space Research, in press, 2000.

Guzik, T.G., et al., Proc. 26th ICRC(Salt Lake City 1999), paper code OG 4.1.03

Schmidt, W.K.H. et al., On the Identification of High Energy Cosmic Ray Electrons in the Advanced Thin Ionization Calorimeter (ATIC), Proc. 26th ICRC(Salt Lake City 1999), paper code OG 4.1.11

Webber, W.R., Source and Acceleration of Cosmic Rays, Space Sci.Rev. 81, 107-142, 1997

Wefel, J. P. et al., The ATIC Experiment: First Flight this conference, 27th ICRC, OG 1.1, 2001

Nishimura, J., et al., Emulsion Chamber Observations of Primary Cosimc-Rays Electrons in the Energy Range 30-1000GeV, ApJ 238, 394, 1980